Adaptive Quantized Control of Flexible Manipulators Subject to Unknown Dead Zones

Zhijia Zhao, *Member, IEEE*, Yiming Liu, Sentao Cai, Zhifu Li, *Member, IEEE*, Yiwen Wang, *Senior Member, IEEE*, Keum-Shik Hong, *Fellow, IEEE*, and Han-Xiong Li, *Fellow, IEEE*

***Abstract*—This article proposes an adaptive control for a flexible manipulator (FM) under the influence of distributed disturbances, unknown dead zones, and input quantization. First, the hybrid effect of the unknown dead zone and input quantization is formulated and represented based on some essential transformations. Then, an adaptive robust quantized control with online updating laws is developed to address the uncertainty of the dead zone, ensure robustness and angle position, and dampen the vibration in the FM system. Subsequently, the Lyapunov theoretical analysis is employed to ensure the bounded stability of the system. Finally, numerical simulations and experiments with a Quanser platform are given to further verify the feasibility and superiority of the designed scheme.**

***Index Terms*—Adaptive control, flexible manipulator (FM), input quantization, unknown dead zone.**

I. Introduction

Flexible manipulators (FMs) play a significant role in numerous applications, such as those related to manufacturing industries, medical operations, and energy exploitation. Therefore, relevant technologies are constantly being developed to meet the complex situations encountered in the operating environment [1], [2], [3]. Owing to their advantages of low cost, low energy, and satisfactory flexibility, FM is higher than that for rigid manipulators. However, the oscillations caused by their flexibility and extrinsic disturbances affect their precise positioning [4], [5]. Therefore, appropriate and effective control methodologies must be developed to achieve vibration inhibition and position tracking of FMs.

Various control technologies have been proposed to attenuate vibration and improve the operation accuracy of FMs. Boundary control exhibits prominent advantages over distributed control and model reduction, such as requiring fewer sensors and actuators and generating no spillover [6]. In recent years, research advances in FM boundary control have been reported. Zhang et al. [7] proposed boundary controllers based on high-gain observers to ensure that the system states such as the position, speed, and vibration constraints were bounded. Liu et al. [8] presented vibration control schemes to eliminate vibrations and perform trajectory tracking in FMs. Facing complex circumstances, researchers have developed more advanced control tactics. Jiang et al. [9] proposed a switching controller to suppress the residual vibration of FMs. In [10], a feedback controller without deformation measurements was designed to address the vibration suppression of FMs. He et al. [11] presented a learning control strategy to realize the satisfactory transient performance of FMs.

Dead-zone nonlinearity, which acts as a static input–output characteristic, inevitably appears when implementing control actuators with the insensitivity to small signals, and severely destroys the system operation [12], [13], [14]. To eliminate undesirable influences, researchers have developed techniques to address dead-zone nonlinearity in flexible systems. The dead zone was separated into a desired control term and a bounded error term in [15], and a desired control law was derived to treat the input nonlinear dead zone in an axial strip system. In [16], robust control strategies were developed to ensure position tracking, vibration abatement, and dead-zone elimination in flexible robots. In [17], adaptive vibration controllers were designed to address uncertainties and compensate for the dead zone in flexible risers. However, the aforementioned studies focused on the dead-zone nonlinearity in flexible systems with known dead-zone parameters; these approaches cannot be applied to systems with unknown dead-zone parameters.

Quantization is inevitable and useful in control systems and has garnered widespread attention as it ensures

Manuscript received 23 December 2022; accepted 29 May 2023. Date of publication 21 June 2023; date of current version 18 September 2023. This work was supported in part by the National Natural Science Foundation of China under Grant 62273112; in part by the Science and Technology Planning Project of Guangzhou City under Grant 202201020185, Grant 202201010758, and Grant 2023A03J0120; in part by the Guangzhou University–Hong Kong University of Science and Technology Joint Research Collaboration Fund under Grant YH202205; in part by the Open Research Fund from the Guangdong Laboratory of Artificial Intelligence and Digital Economy (Shenzhen) under Grant GML-KF-22-27; and in part by the National Research Foundation of Korea under the Ministry of Science and ICT, South Korea, under Grant RS-2023-00207954. This article was recommended by Associate Editor W. Sun. *(Corresponding author: Zhifu Li.)*

Zhijia Zhao, Yiming Liu, Sentao Cai, and Zhifu Li are with the School of Mechanical and Electrical Engineering and the Guangdong–Hong Kong–Macao Key Laboratory of Multi-Scale Information Fusion and Collaborative Optimization Control of Complex Manufacturing Process, Guangzhou University, Guangzhou 510006, China, and also with the Guangdong Laboratory of Artificial Intelligence and Digital Economy (Shenzhen), Shenzhen 518060, China (e-mail: zhjzhaoscut@163.com; 1032385189@qq.com; 2112007142@e.gzhu.edu.cn; lizhifu8@163.com).

Yiwen Wang is with the Department of Electronic and Computer Engineering and the Department of Chemical and Biological Engineering, The Hong Kong University of Science and Technology, Hong Kong (e-mail: eewangyw@ust.hk).

Keum-Shik Hong is with the School of Mechanical Engineering, Pusan National University, Busan 46241, Republic of Korea (e-mail: kshong@pusan.ac.kr).

Han-Xiong Li is with the Department of Advanced Design and Systems Engineering, City University of Hong Kong, Hong Kong (e-mail: mehxli@cityu.edu.hk).

Color versions of one or more figures in this article are available at https://doi.org/10.1109/TSMC.2023.3283268.

Digital Object Identifier 10.1109/TSMC.2023.3283268

sufficient precision and requires a low communication rate [18], [19], [20]. Recently, considerable progress has been fulfilled in the quantized control of nonlinear or linear systems. In [21], input quantization was decomposed into a new nonlinear function, and fuzzy-logic techniques were used to design a fuzzy adaptive tracking controller. In [22], a robust tracking control was designed using a sector-bounded quantizer to stabilize uncertain nonlinear systems. In [23], a state estimator was designed to solve the intrinsic quantization error of the quantized state and stabilize the control performance. The aforementioned studies were confined to designing the quantization control of ordinary differential equation (ODE) systems; these strategies are not directly applicable to partial differential equation (PDE) flexible systems. Recently, new advances have been made in the quantization control for flexible systems. Gao and Liu [24] exploited an NN to resolve the vibration inhibition problem of a flexible wing with unknown disturbances and input quantization. Wang and Liu [25] presented a relative threshold strategy in an FM system considering communication capacity constraints during signal transmission and communication loading. In [26], a bilateral coordination quantization control scheme was developed to realize the stability of a leader/follower flexible system. However, these studies were limited to the quantization control of flexible systems because the unknown dead zone was neglected. Successful solutions for the quantization control of flexible systems have been established, but a control design for an FM with an unknown dead zone and input quantization is yet to be developed.

In this article, we address the vibration attenuation and tracking control of FMs with an unknown dead zone and input quantization. The major contributions of this study are summarized as follows.

1) An adaptive quantized controller with online updating laws is proposed to resolve the dead zone and uncertainty compensation, stabilize the vibration and angle position, and achieve robustness in the FM system.
2) Compared with the NN controller that suppresses the vibration of an FM with an input dead zone in [27], the dynamic model proposed is constructed by PDEs that is more accurate and contains all motion modes of the system. Furthermore, the designed strategy reduces the convergence time of the system output state from 5 to 2 s.
3) The system's bounded stability is investigated using the direct Lyapunov method, and numerical simulations and experiments are conducted on a Quanser platform to validate the control performance.

II. Problem Formulation and Preliminaries

A. System Model

A simple FM model is presented in Fig. 1. Here, z, t, and L denote the independent space, time, and length of the manipulator, respectively. The FM is subjected to a time-varying disturbance $F(z,t)$, and the control torque $\tau(t)$ arises at the manipulator's initial position. The displacement $\kappa(z,t)$ is deduced as $\kappa(z,t)=\alpha(z,t)+z\theta(t)$, where $\alpha(z,t)$ and $\theta(t)$

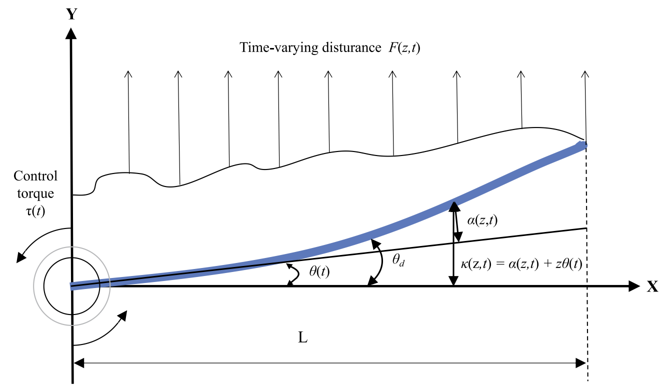

Fig. 1. FM system.

denote the system's elastic deflection and the hub's angle position, respectively. θ_d describes a desired angle in the working environment.

Remark 1: In this article, the following notations are used for concise expressions: $(\star)=(\star)(z,t)$, $(\star)'=\partial(\star)/\partial z$, $(\star)''=\partial^2(\star)/\partial z^2$, $(\star)'''=\partial^3(\star)/\partial z^3$, $(\star)''''=\partial^4(\star)/\partial z^4$, $(\dot{\star})=\partial(\star)/\partial t$, $(\ddot{\star})=\partial^2(\star)/\partial t^2$, $(\star)_0=(\star)(0,t)$, and $(\star)_L=(\star)(L,t)$.

The governing equation of an FM is given by [28]

$$\rho\ddot{\kappa}=-EI\alpha''''+T\kappa''-c\dot{\kappa}+F(z,t)\,\forall z\in[0,L] \tag{1}$$

with c, T, EI, and ρ being the damping coefficient, tension, bending stiffness, and density of the FM, respectively.

The state $\alpha(z,t)$ has the following boundary conditions:

$$\alpha_0=\alpha_0'=\alpha_L'=0 \tag{2}$$
$$T\alpha_L'=EI\alpha_L''' \tag{3}$$

and the kinetics of $\theta(t)$ is obtained as

$$I\ddot{\theta}-EI\alpha_0''-T\alpha_L=\tau(t) \tag{4}$$

with I denoting the FM's hub inertia.

Assumption 1: The time-varying disturbance $F(z,t)$ satisfies $|F(z,t)|\le\bar{F}\ \forall(z,t)\in[0,L]\ \times[0,+\infty)$, with $\bar{F}\in\mathbb{R}^+$ as a constant. This assumption is deemed to be rational owing to the finite energy of $F(z,t)$.

B. Input Quantization

In quantization control, the common quantizers are hysteresis and logarithmic quantizers. In this study, we selected the hysteresis quantizer to design the controller, which is advantageous to avoid chattering with the more accurate quantization levels. The hysteresis quantizer was described in [18] as follows:

$$Q(u(t))=\begin{cases} u_i\mathrm{sgn}(u), & \text{if } \frac{u_i}{1+\delta}<|u|\le u_i,\ \dot{u}<0, \text{ or}\\ & u_i<|u|\le\frac{u_i}{1-\delta},\ \dot{u}>0\\ u_i(1+\delta)\mathrm{sgn}(u), & \text{if } u_i<|u|\le\frac{u_i}{1-\delta},\ \dot{u}<0, \text{ or}\\ & \frac{u_i}{1-\delta}<|u|\le\frac{u_i(1+\delta)}{1-\delta},\ \dot{u}>0\\ 0, & \text{if } 0\le|u|<\frac{u_{\min}}{1+\delta},\ \dot{u}<0, \text{ or}\\ & \frac{u_{\min}}{1+\delta}\le|u|<u_{\min},\ \dot{u}>0\\ Q\big(u(t^-)\big), & \text{if } \dot{u}=0 \end{cases} \tag{5}$$

where $u(t)$ is the control input, $u_i = \varepsilon^{(1-y)} u_{\min}$ with $y = 1, 2, \ldots$, $\delta = (1 - \varepsilon/1 + \varepsilon)$ with $0 < \varepsilon < 1$, $u_{\min} > 0$ denotes the dead zone of the quantization output.

C. Unknown Dead-Zone Nonlinearity

The mathematical expression of the dead-zone nonlinearity proposed is given as follows:

$$D(v(t)) = \begin{cases} g(v - l_1), & \text{if } \ v > l_1 \\ 0, & \text{if } l_2 \leq v \leq l_1 \\ g(v - l_2), & \text{if } \ v < l_2 \end{cases} \tag{6}$$

where $D(\star)$ represents a dead-zone input, $v(t)$ describes a designed controller, g represents an unknown scale factor, and $l_1 > 0$ and $l_2 < 0$ represent the width parameters of the nonlinearity.

D. Preliminaries

The following lemmas facilitate the subsequent analysis.

Lemma 1: Let $\iota_1(z, t), \iota_2(z, t) \in \mathbb{R}$ be defined on $(z, t) \in [0, L] \times [0, +\infty)$. Then, we then arrive at [17]

$$\iota_1 \iota_2 \leq \varrho \iota_1^2 + \frac{1}{\varrho} \iota_2^2 \tag{7}$$

where ϱ is a positive constant.

Lemma 2: If the condition $\iota(0, t) = 0$ is satisfied, the following inequalities hold [15]:

$$\iota^2 \leq L \int_0^L \iota'^2 dz \tag{8}$$

$$\int_0^L \iota^2 dz \leq L^2 \int_0^L \iota'^2 dz. \tag{9}$$

Lemma 3: The following inequality for $\Delta(t) \in \mathbb{R}$ has [29]:

$$0 \leq |\Delta(t)| - \Delta(t) \tanh\left[\frac{\Delta(t)}{\psi}\right] \leq \psi \Lambda \tag{10}$$

with $\Lambda = 0.2785$ and $\psi > 0$.

III. Control Design

In this study, an adaptive robust quantized controller is constructed. The control method not only tracks the deflection angle of the manipulator and suppresses the manipulator's vibration but also considers the nonlinear characteristics of a dead zone with unknown parameters. Furthermore, the input signal is hysteresis quantized to reduce the communication burden, which makes the design of the controller more challenging. A block diagram of the proposed scheme for the FM system is shown in Fig. 2.

A. Adaptive Robust Control

Before designing the controller, we first synthesize the effect of the unknown nonlinearity and input quantization into system input $\tau(t)$. Using some transforms described in [30], we formulated the expression of $\tau(t)$ as

$$\tau(t) = g q_1(t) u_d(t) + g q_2(t) + r \tag{11}$$

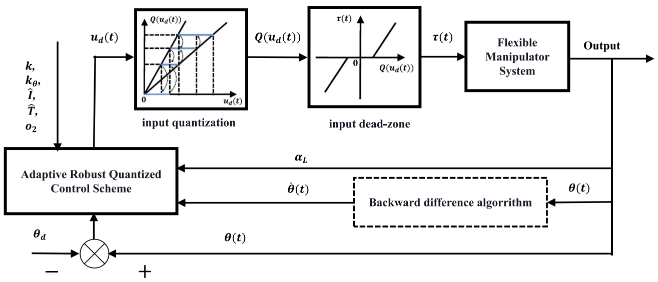

Fig. 2. Adaptive robust quantized control design for the FM.

where $u_d(t)$ is the desired control to be presented in the subsequent design. $q_1(t)$, $q_2(t)$, and r are defined as follows:

$$q_1(t) = \begin{cases} \frac{Q(u_d)}{u_d}, & \text{if } |u_d(t)| \geq d \\ 1, & \text{if } |u_d(t)| < d \end{cases} \tag{12}$$

$$q_2(t) = \begin{cases} 0, & \text{if } |u_d(t)| \geq d \\ Q(u_d) - u_d, & \text{if } |u_d(t)| < d \end{cases} \tag{13}$$

$$r = \begin{cases} -g l_1, & \text{if } \ q_1(t) u_d(t) + q_2(t) > l_1 \\ -g q_1(t) u_d - g q_2(t), & \text{if } l_2 \leq q_1(t) u_d(t) + q_2(t) \leq l_1 \\ -g l_2, & \text{if } \ q_1(t) u_d(t) + q_2(t) < l_2 \end{cases} \tag{14}$$

where d is defined as the width of the dead zone for $Q(u_d)$ and $d > 0$. Because the symbol is immutable in the quantization process, we can derive that $q_1(t) > 0$ from (12). If $|u_d(t)| < d$, then $Q(u_d)$ is bounded. Therefore, we know that $q_2(t)$ is bounded, thus satisfying $|q_2(t)| < \bar{q}_2$ with constant $\bar{q}_2 > 0$. Meanwhile, according to [17, Remark 1], $|r| \leq \bar{r}$ with constant $\bar{r} > 0$.

Remark 2: Considering the quantization factor, the expression of the control signal is more complex. If it is not processed, it increases the difficulty in designing the controller. Therefore, based on the dead-time characteristic of quantization, we express the control signal in a simple form through (12) and (13).

Based on the above analysis, (4) is formulated as

$$I\ddot{\theta} - EI\alpha_0'' - T\alpha_L = g q_1(t) u_d(t) + g q_2(t) + r. \tag{15}$$

Let $q = g q_1(t)$ and $e_1 = 1/q_{\min}$, where $q_{\min}$ is the lower bound of q. Similarly, $e_2 = g\bar{q}_2$ exists. Then, we define some estimated values $\hat{e}_1$ and $\hat{\bar{r}}$ of e_1 and $\bar{r}$, with the estimated errors defined as $\tilde{e}_1 = \hat{e}_1 - e_1$ and $\tilde{\bar{r}} = \hat{\bar{r}} - \bar{r}$.

Considering the organization of (15), we introduce an auxiliary signal $n(t)$ as

$$\begin{aligned} n(t) = k u_a(t) + \hat{I}\beta\dot{\theta}(t) + \hat{T}\alpha_L + k_1 \alpha_L \\ + k_\theta \theta_n(t) + \tanh\left[\frac{u_a(t)}{o_2}\right] \hat{\bar{r}} \end{aligned} \tag{16}$$

with $\beta > 0$, $\theta_n(t) = [\theta(t) - \theta_d]$ being a tracking error, and $u_a(t) = \dot{\theta}(t) + \beta \theta_n(t)$.

Then, the desired controller $u_d(t)$ is designed as

$$u_d(t) = -\frac{\hat{e}_1^2 n^2(t) u_a(t)}{|\hat{e}_1 n(t) u_a(t)| + w} \tag{17}$$

where $w > 0$.

We then construct the following adaptive laws as:

$$\dot{\hat{e}}_1 = \mu_1 u_a(t) n(t) - \mu_1 \mu_2 \hat{e}_1 \tag{18}$$

$$\dot{\hat{I}} = \mu_3 u_a(t) \beta \dot{\theta}(t) - \mu_3 \mu_4 \hat{I} \tag{19}$$

$$\dot{\hat{\bar{r}}} = \mu_5 u_a(t) \tanh\left[\frac{u_a(t)}{o_2}\right] - \mu_5 \mu_6 \hat{\bar{r}} \tag{20}$$

$$\dot{\hat{T}} = \mu_7 u_a(t) \alpha_L - \mu_7 \mu_8 \hat{T} \tag{21}$$

where $\mu_i > 0$, $i = 1, 2, \ldots, 8$.

Remark 3: The advantage of the proposed controller in comparison with the existing ones is that it needs only the state information of the deflection angle of the manipulator, and the unmeasurable states can be estimated with the presented adaptive laws.

B. Stability Proof

The Lyapunov function is selected as

$$\Omega(t) = \Omega_1(t) + \Omega_2(t) + \Omega_3(t) + \eta(t) \tag{22}$$

where

$$\Omega_1(t) = \frac{1}{2}\rho \int_0^L \dot{\kappa}^2 dz + \frac{1}{2} EI \int_0^L \alpha''^2 dz + \frac{1}{2} T \int_0^L \alpha'^2 dz \tag{23}$$

$$\Omega_2(t) = \frac{1}{2} I {u_a}^2(t) + \frac{1}{2} k_{\theta[\theta(t)-\theta_d]^2} \tag{24}$$

$$\Omega_3(t) = \beta\rho \int_0^L \dot{\kappa}\kappa_e dz \tag{25}$$

$$\eta(t) = \frac{1}{2\mu_1 e_1}\tilde{e}_1^2 + \frac{1}{2\mu_3}\tilde{I}^2 + \frac{1}{2\mu_5}\tilde{\bar{r}}^2 + \frac{1}{2\mu_7}\tilde{T}^2 \tag{26}$$

in which $\kappa_e = \alpha + z[\theta(t) - \theta_d]$ and we obtain $\dot{\kappa}_e = \dot{\kappa}$.

Lemma 4: The Lyapunov function (22) satisfies

$$0 \le \gamma_1[\Omega_1(t) + \Omega_2(t) + \eta(t)] \le \Omega(t) \le \gamma_2[\Omega_1(t) + \Omega_2(t) + \eta(t)] \tag{27}$$

where $\gamma_1, \gamma_2 > 0$.

Proof: See Appendix A. ■

Lemma 5: The time derivative of (22) is upper bounded as

$$\dot{\Omega}(t) \le -\gamma\Omega(t) + \epsilon \tag{28}$$

where $\gamma, \epsilon > 0$.

Proof: See Appendix B. ■

Theorem 1: For the FM system modeled in (1)–(4), adopting the constructed adaptive quantized control tactics (16)–(21) with the initial conditions and the appropriate control gains to satisfy inequalities (44)–(49), the following properties are obtained, which manifests the uniformly ultimate boundedness of the FM system.

1) The elastic offset $\alpha(z, t)$ is guaranteed to converge to set Ξ_1

$$\Xi_1 := \left\{\alpha(z, t) \in \mathbf{R} \middle| \lim_{t\to\infty} |\alpha(z, t)| \le \sqrt{\frac{2L\epsilon}{\beta T\gamma_1\gamma}} \quad \forall z \in [0, L]\right\}. \tag{29}$$

2) The tracking error eventually converges to set Ξ_2

$$\Xi_2 := \left\{\theta_n(t) \in \mathbf{R} \middle| \lim_{t\to\infty} |\theta_n(t)| \le \sqrt{\frac{2\epsilon}{k_\theta\gamma_1\gamma}}\right\}. \tag{30}$$

Proof: See Appendix C. ■

Remark 4: In the process of stability proof, we deduced some constraint conditions as (44)–(50) that the parameter settings must satisfy. We first select a set of appropriate parameters of σ_1, σ_4, σ_5, and β to make (44) hold. Then, we can infer the value range of σ_2 in (46). The settings of σ_6, σ_7, k, and k_1 need to constantly adjust to satisfy the inequality (47) and (48). Finally, the values of σ_3 and k_θ can be derived. During the parameter adjusting in simulation, appropriate values of k, k_1, k_θ, and β are suitably tuned until excellent transient and steady-state performance is derived.

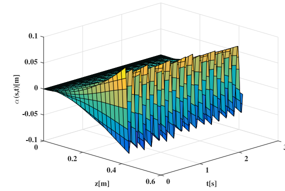

Fig. 3. Deflection $\alpha(z, t)$ of the FM without control.

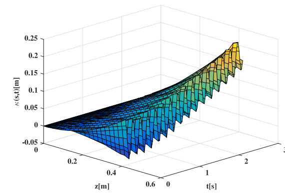

Fig. 4. Displacement $\kappa(z, t)$ of the FM without control.

IV. Numerical Simulation

Simulations were conducted to verify the control performance of the designed strategy. Finite difference algorithms were applied to model the operation of the FM system. The system parameters were $L = 0.419$ m, $EI = 0.157$ Nm^2, $T = 0.01$ N, $I = 0.0038$ kg/m^2, $c = 0.02$ NS/m, and $\rho = 0.1$ kg/m [31]. The initial vibration values of the FM were $\alpha(z, 0) = 0.5z^2$ and $\dot{\alpha}(z, 0) = 0$. The existent distributed disturbance was defined as $F(z, t) = [0.6 + \sin(\pi zt) + \sin(2\pi zt) + \sin(3\pi zt)] \times (z/100)$. In the simulations, we selected the desired trajectory $\theta_d = 15°$ and the dead-zone characteristics as $g = 1$, $l_1 = 0.2$, and $l_2 = -0.2$. The simulation results of the FM in the following four cases were considered to analyze the dynamic process with different schemes.

Without Control: The dynamics of the FM under no control are depicted in Fig. 3, and it is evident that the flexible link suffers from periodically sustained oscillations. As shown in Fig. 4, the total deflection of the FM gradually increases with the deflection angle as expected.

With the Proposed Control Scheme: We set the control gains as $k = 10$, $k_\theta = 90$, $\beta = 0.18$, $k_1 = 0.1$, $o_2 = 0.01$, and $w = 0.01$. Furthermore, we applied the proposed control (17)

TABLE I
COMPARISON OF THREE CONTROL METHODS IN SIMULATION

Methods	Angular position			End-point deflection		
	Overshoot	Accommodation time	Steady-state error	Max	Peak-to-peak	Steady
Proposed control	3.78%	0.6890 s	0.0004 rad	0.0878 m	0.1691 m	0.0019 m
PID control	N/A	1.3093 s	0.0018 rad	0.0878 m	0.1622 m	0.0034 m
Adaptive control	N/A	1.5533 s	0.0010 rad	0.0878 m	0.1590 m	0.0028 m

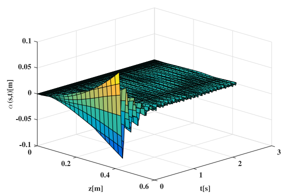

Fig. 5. Deflection $\alpha(z, t)$ of the FM with adaptive quantized control.

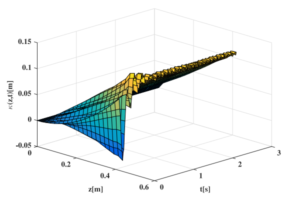

Fig. 6. Displacement $\kappa(z, t)$ of the FM with adaptive quantized control.

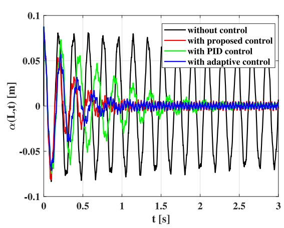

Fig. 7. End-point deflection of the FM.

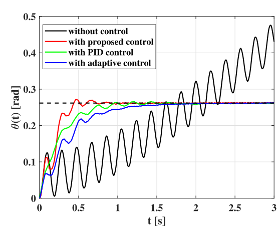

Fig. 8. Angular position of the FM.

to the FM system. The control results obtained are shown in Figs. 5 and 6. The deflection $\alpha(L, t)$ of the FM gradually converges from 0.088 m to approximately 0.02 m within 1 s after the operation and then converges to the minimal neighborhood of 0 to reach stability. The deflection position of the manipulator $\theta(t)$ tracks the neighborhood of the desired trajectory position with a large range of motion in 1 s and finally coincides with the desired trajectory. Both become stable in 3 s and exhibit effective real-time performance. The output state variables are depicted in Figs. 7 and 9, in which $\kappa(L, t)$, $\alpha(z, t)$, and $\theta(t)$ are represented by a red solid line.

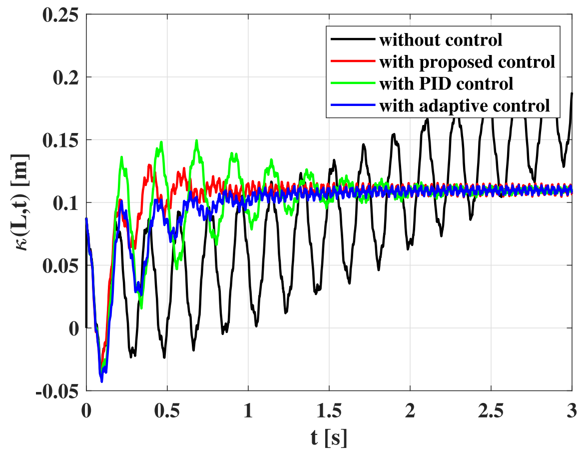

Fig. 9. Displacement of the FM.

With the PID Control Scheme: For comparison purposes, we set a PID control described as $u1(t) = -k_p[\theta(t) - \theta_d] - k_d\dot{\theta}(t) - k_i \int_0^T [\theta(t) - \theta_d]dt$ by selecting the control gains as $k_p = 20$, $k_i = 0.01$, and $k_d = 5$. The control performance is indicated by a green solid line in Figs. 7 and 9. The relevant criterion of the control result is summarized in Table I. From Fig. 7, we can conclude that this method takes twice as long to suppress the end amplitude as the former. In position tracking, the deflection speed of the manipulator is slightly low, and it takes 0.69 s to track to the desired trajectory, as shown in Fig. 8.

With the Adaptive Scheme: To highlight the superiority of the designed controllers with an unknown dead zone and quantization, we referred to [32] to set an adaptive control strategy without considering the above-mentioned nonlinear characteristics. The controller is described as $u2(t) = -ku_a(t) - [k_1 + \hat{T}(t)]\alpha(L, t) - \hat{I}(t)\beta\dot{\theta} - k_\theta[\theta(t) - \theta_d]$ by selecting the control gains as $k = 1.8$, $k_1 = 0.01$, $\beta = 0.02$, and $k_\theta = 4.7$, with adaptive laws as $\dot{\hat{T}}(t) = a_1\alpha(L, t)u_a(t) - a_1a_2\hat{T}(t)$ and $\dot{\hat{I}}(t) = a_3\beta\dot{\theta}(t)u_a(t) - a_3a_4\hat{I}(t)$. The simulation result is represented by the blue solid line in Figs. 7 and 9. It is apparent that this method can suppress the end-point vibration as rapidly as the proposed scheme, but the control effect of tracking the desired position is worse than that of the above-mentioned methods with a convergence time of 1.55 s, as shown in Fig. 8.

Furthermore, we compared the designed control signal with the quantization input signal as shown in Fig. 10, from which we conclude that the control signal after dead zone and quantization has superior convergence. The quantization input signal is described in Fig. 11. Through comparison with the other two methods, the proposed scheme is found to exhibit a fast convergence speed and stable control accuracy. The simulation

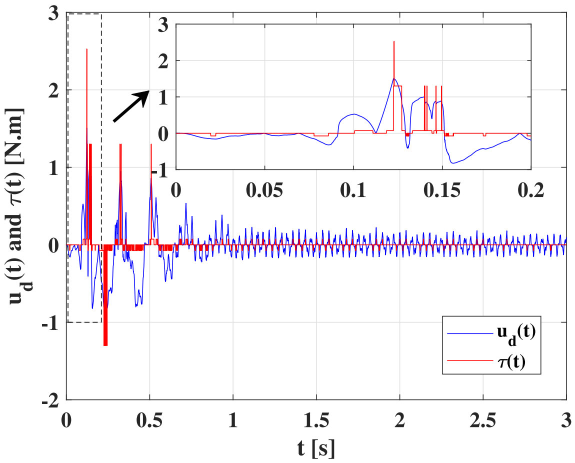

Fig. 10. Designed control signal and quantized control signal.

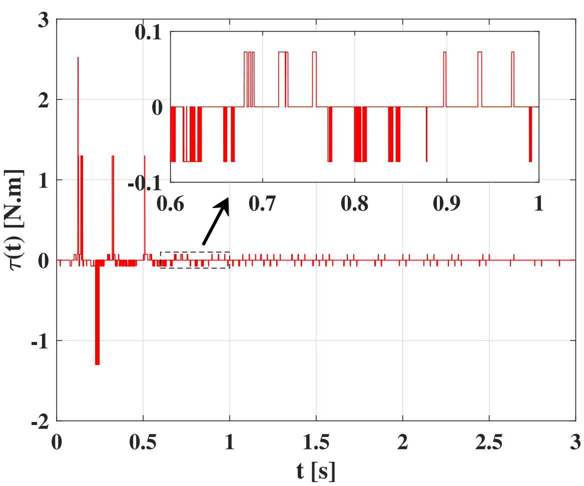

Fig. 11. Quantized control signal.

results agree closely with those of the stability analysis and validate the feasibility of the designed quantized control.

V. Experimental Verification

An experimental platform was established, as shown in Fig. 12, to further validate the proposed control strategy. The experimental platform was originally developed by Quanser Inc. and comprises a rotary flexible link, strain gauge, controller, servomotor drive unit power, amplifier, and filter. A dc motor rotates the flexible link in the horizontal plane, and an installed strain gauge detects the deflection of the tip in the end of the motor.

Before performing the experiments, we conducted a test of the dead zone in this platform. We concluded that the actuator did not operate when we applied an input signal from −0.2 to 0.1 V. Then, we built Simulink modules according to our control scheme. On the physical platform, we also conducted experiments on the other two methods mentioned in the simulation to verify the superiority of the designed strategy, and the control effects are shown in Figs. 13 and 14. The relevant criterion of the control result is summarized in Table II. From Fig. 13, adopting the proposed strategy, the FM system only takes 0.35 s to reach the neighborhood of the desired trajectory

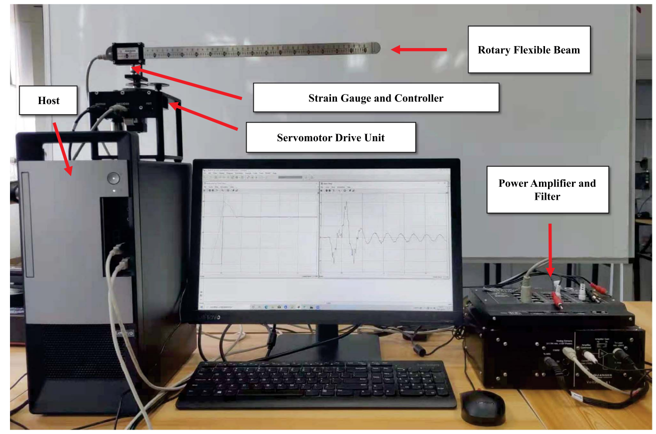

Fig. 12. Rotary flexible link system.

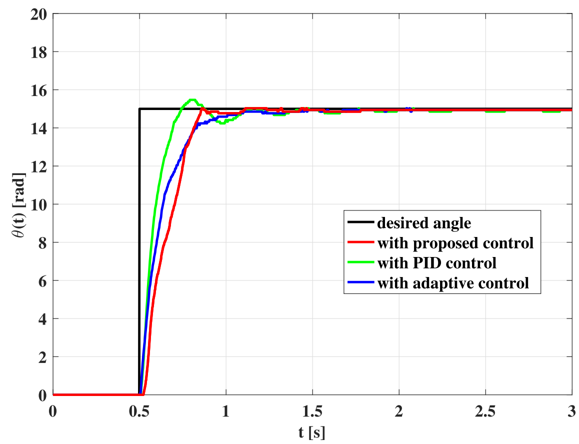

Fig. 13. Angular position $\theta(t)$ with the proposed control.

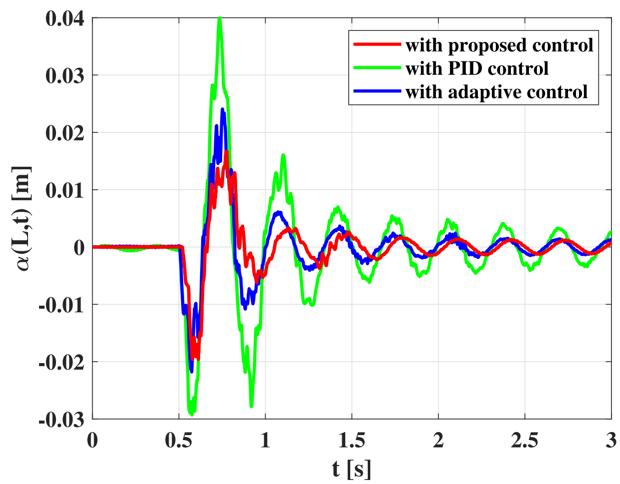

Fig. 14. Tip deflection $\alpha(L, t)$ with the proposed control.

with almost no overshoot. From Fig. 14, compared with other control methods, the proposed scheme can effectively suppress the vibration of FM. Further, we can conclude from the experimental processes that the proposed control better positions the FM at the desired angle, stabilizes the offset at a small neighborhood around zero, and disposes of the unknown dead zone and quantization, verifying the validity and effectiveness of the theory. The system control input $\tau(t)$ is shown in Fig. 15.

TABLE II
COMPARISON OF THREE CONTROL METHODS IN EXPERIMENT

Methods	Angular position			Tip deflection		
	Overshoot	Accommodation time	Steady-state error	Max	Peak-to-peak	Steady
Proposed control	0.20%	0.8505 s	0.0586 rad	0.0195 m	0.0355 m	0.0011 m
PID control	3.12%	1.3403 s	0.1465 rad	0.0400 m	0.0793 m	0.0031 m
Adaptive control	N/A	1.0607 s	0.0586 rad	0.0240 m	0.0557 m	0.0014 m

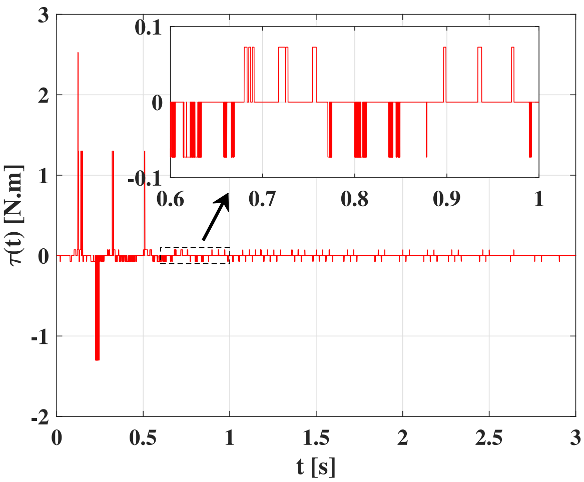

Fig. 15. Control input $\tau(t)$ with the proposed control.

VI. CONCLUSION

This article proposed an adaptive robust quantized scheme for an FM system against the effects of an unknown dead zone, input quantization, and external disturbances. An adaptive robust quantized control framework was established to restrain the flexible vibration, cope with the unknown dead zone and quantization, eliminate the uncertainty, and realize localization in the FM. By decomposing the nonlinear elements of the FM system, an adaptive control law was designed to estimate and compensate the bounded part of the nonlinearity. The designed strategy guaranteed that the elastic deformation of the FM stabilizes to a minimal interval of zero, and the trajectory tracking was simultaneously fulfilled. Through analysis of the theoretical, simulation, and experimental results, stable control results are effectively verified. Future work will focus on the applicability verification when the controlled target object is multilink FM. In addition, we will consider the effect of the state and output quantization problem and attempt to develop relevant control strategies in the FM system.

APPENDIX A

Using Lemmas 1 and 2 to (25), we obtain

$$\begin{aligned}|\Omega_3(t)| &\le \beta\rho\int_0^L |\dot{\kappa}\alpha|dz + \beta\rho\int_0^L L|\dot{\kappa}[\theta(t)-\theta_d]|dz \\ &\le \frac{\beta\rho(1+L)}{2}\int_0^L \dot{\kappa}^2 dz + \frac{\beta\rho L^2}{2}\int_0^L \alpha'^2 dz \\ &\quad + \frac{\beta\rho L}{2}\theta_n^2(t) \le \chi_1[\Omega_1(t)+\Omega_2(t)] \end{aligned} \tag{31}$$

where $\chi_1 = \beta\max[\rho(1+L), \frac{\beta L^2}{T}, \frac{\rho L}{k_\theta}]$. Then, we have

$$\begin{aligned}(1-\chi_1)[\Omega_1(t)+\Omega_2(t)] &\le \Omega_1(t)+\Omega_2(t)+\Omega_3(t) \\ &\le (1+\chi_1)[\Omega_1(t)+\Omega_2(t)]. \end{aligned} \tag{32}$$

Considering (26) yields

$$\gamma_1[\Omega_1(t)+\Omega_2(t)+\eta(t)] \le \Omega(t) \le \gamma_2[\Omega_1(t)+\Omega_2(t)+\eta(t)] \tag{33}$$

where $\gamma_1 = \min[1-\chi_1, 1]$ and $\gamma_2 = \max[1+\chi_1, 1]$, respectively.

APPENDIX B

The time derivative of (22) is obtained as

$$\dot{\Omega}(t) = \dot{\Omega}_1(t) + \dot{\Omega}_2(t) + \dot{\Omega}_3(t) + \dot{\eta}(t). \tag{34}$$

The first term of (34) yields

$$\dot{\Omega}_1(t) = \rho\int_0^L \dot{\kappa}\ddot{\kappa}dz + EI\int_0^L \alpha''\dot{\alpha}''dz + T\int_0^L \alpha'\dot{\alpha}'dz. \tag{35}$$

From the dynamical model (1)–(3), integrating results in

$$\begin{aligned}\dot{\Omega}_1(t) &\le -EI\dot{\theta}(t)\alpha_0'' - T\dot{\theta}(t)\alpha_L - (c-\sigma_1)\int_0^L \dot{\kappa}^2 dz \\ &\quad + \frac{1}{\sigma_1}\int_0^L F^2(z,t)dz \end{aligned} \tag{36}$$

where $\sigma_1 > 0$.

The second term of (32) yields

$$\dot{\Omega}_2(t) = Iu_a(t)\dot{u}_a^2(t) + k_\theta\dot{\theta}(t)[\theta(t)-\theta_d]. \tag{37}$$

Combining (15) and (17) yields

$$\begin{aligned}\dot{\Omega}_2(t) = u_a(t)\Bigg[&EI\alpha_0'' + T\alpha_L + I\beta\dot{\theta}(t) + gq_2(t) + r \\ &- gq_1(t)\frac{u_a(t)\hat{e}_1^2 n^2(t)}{|u_a(t)\hat{e}_1 n(t)| + w}\Bigg] \\ &+ k_\theta\dot{\theta}(t)[\theta(t)-\theta_d]. \end{aligned} \tag{38}$$

Invoking (16) and using the substitution variables, (36) can be rewritten as

$$\begin{aligned}\dot{\Omega}_2(t) \le u_a(t)\Bigg[&n(t) - ku_a(t) + EI\alpha_0'' + T\alpha_L - \hat{T}\alpha_L - k_1\alpha_L \\ &+ I\beta\dot{\theta}(t) - \hat{I}\beta\dot{\theta}(t) - k_\theta[\theta(t)-\theta_d] - \tanh\left[\frac{u_a(t)}{o_2}\right]\hat{\bar{r}} \\ &- q\frac{u_a(t)\hat{e}_1^2 n^2(t)}{|u_a(t)\hat{e}_1 n(t)| + w} + e_2 + \bar{r}\Bigg] + k_\theta\dot{\theta}(t)\theta_n(t)\end{aligned}$$

$$\begin{aligned}&\leq u_a(t)n(t) - k{u_a}^2(t) + u_a(t)EI\alpha_0'' - u_a(t)\tilde{T}\alpha_L\\ &- u_a(t)k_1\alpha_L - u_a(t)\tilde{I}\beta\dot{\theta}(t) - k_\theta\beta\theta_n^2(t)\\ &- u_a(t)\tanh\left[\frac{u_a(t)}{o_2}\right]\hat{\bar{r}} + \frac{w}{e_1} - \frac{u_a(t)\hat{e}_1 n(t)}{e_1}\\ &+ u_a(t)e_2 + u_a(t)\bar{r}.\end{aligned} \tag{39}$$

$\dot{\Omega}_3(t)$ of (34) is derived as

$$\dot{\Omega}_3(t) = \beta\rho\int_0^L \ddot{\kappa}\kappa_e dz + \beta\rho\int_0^L \dot{\kappa}\dot{\kappa}_e dz. \tag{40}$$

Applying $\kappa_e = \alpha + z\theta_n(t)$ yields

$$\begin{aligned}\dot{\Omega}_3(t) &\leq -\beta EI\theta_n(t)\alpha_0'' - \beta T\theta_n(t)\alpha_L - \left(\beta EI - \sigma_2\beta L^4\right)\\ &\int_0^L {\alpha''}^2 dz - \left(\beta T - \frac{\beta cL^2}{\sigma_4}\right)\int_0^L {\alpha'}^2 dz\\ &+ (\beta\rho + \beta c\sigma_4 + \beta cL\sigma_5)\int_0^L \dot{\kappa}^2 dz + \left(\frac{\beta cL}{\sigma_5} + \sigma_3\beta L^2\right)\\ &\theta_n^2(t) + \left(\frac{\beta}{\sigma_2} + \frac{\beta}{\sigma_3}\right)\int_0^L F^2(z,t)dz.\end{aligned} \tag{41}$$

The fourth term of (34) is given by

$$\dot{\eta}(t) = \frac{1}{\mu_1 e_1}\tilde{e}_1\dot{\hat{e}}_1 + \frac{1}{\mu_3}\tilde{I}\dot{\hat{I}} + \frac{1}{\mu_5}\tilde{\bar{r}}\dot{\hat{\bar{r}}} + \frac{1}{\mu_7}\tilde{T}\dot{\hat{T}}. \tag{42}$$

Invoking (18)–(21) obtains

$$\begin{aligned}\dot{\eta}(t) \leq\ &\frac{u_a(t)\tilde{e}_1}{e_1}n(t) - \frac{\mu_2}{2e_1}\tilde{e}_1^2 + \frac{\mu_2}{2}e_1 - \frac{\mu_8}{2}\tilde{T}^2 + \frac{\mu_8}{2}T^2\\ &+ u_a(t)\tilde{I}\beta\dot{\theta}(t) - \frac{\mu_4}{2}\tilde{I}^2 + \frac{\mu_4}{2}I^2 + u_a(t)\tilde{T}\alpha_L\\ &+ u_a(t)\tanh\left[\frac{u_a(t)}{o_2}\right]\tilde{\bar{r}} - \frac{\mu_6}{2}\tilde{\bar{r}}^2 + \frac{\mu_6}{2}\bar{r}^2.\end{aligned} \tag{43}$$

By substituting (36), (39), (41), and (43) into (34), $\dot{\Omega}(t)$ can be derived as

$$\begin{aligned}\dot{\Omega}(t) \leq\ &-(c - \sigma_1 - \beta\rho - \beta c\sigma_4 - \beta cL\sigma_5)\int_0^L \dot{\kappa}^2 dz\\ &- \left(\beta EI - \sigma_2\beta L^4\right)\int_0^L {\alpha''}^2 dz + \frac{w}{e_1} + \frac{\mu_8}{2}T^2\\ &- \left[\beta T - \frac{\beta cL^2}{\sigma_4} - \sigma_6(T+k_1)L\right]\int_0^L {\alpha'}^2 dz + \frac{\mu_2}{2}e_1\\ &- \left(k - \frac{T+k_1}{\sigma_6} - \sigma_7\right){u_a}^2(t) + \frac{1}{\sigma_7}{e_2}^2 + \frac{\mu_4}{2}I^2\\ &- \left(k_\theta\beta - \frac{\beta cL}{\sigma_5} + \sigma_3\beta L^2\right)\theta_n^2(t) + 0.2785\bar{r}o_2\\ &- \frac{\mu_2}{2e_1}\tilde{e}_1^2 - \frac{\mu_4}{2}\tilde{I}^2 - \frac{\mu_6}{2}\tilde{\bar{r}}^2 - \frac{\mu_8}{2}\tilde{T}^2 + \frac{\mu_6}{2}\bar{r}^2\\ &+ \left(\frac{1}{\sigma_1} + \frac{\beta}{\sigma_2} + \frac{\beta}{\sigma_3}\right)\int_0^L F^2(z,t)dz\end{aligned} \tag{44}$$

where $\sigma_2, \sigma_3 > 0$, and the gains k, k_θ, k_1, o_2, β, and μ_i, $i = 1, 2, \ldots, 8$ are selected to satisfy the following:

$$\zeta_1 = c - \sigma_1 - \beta\rho - \beta c\sigma_4 - \beta cL\sigma_5 > 0 \tag{45}$$

$$\zeta_2 = \beta EI - \sigma_2\beta L^4 > 0, \quad \zeta_6 = \frac{\mu_2}{2e_1} > 0 \tag{46}$$

$$\zeta_3 = \beta T - \frac{\beta cL^2}{\sigma_4} - \sigma_6(T+k_1)L > 0, \quad \zeta_7 = \frac{\mu_4}{2} > 0 \tag{47}$$

$$\zeta_4 = k - \frac{T+k_1}{\sigma_6} - \sigma_7 > 0, \quad \zeta_8 = \frac{\mu_6}{2} > 0 \tag{48}$$

$$\zeta_5 = k_\theta\beta - \frac{\beta cL}{\sigma_5} + \sigma_3\beta L^2 > 0, \quad \zeta_9 = \frac{\mu_8}{2} > 0 \tag{49}$$

$$\begin{aligned}\epsilon =\ &\frac{w}{e_1} + \frac{\mu_2}{2}e_1 + \frac{\mu_4}{2}I^2 + 0.2785\bar{r}o_2 + \frac{\mu_6}{2}\bar{r}^2 + \frac{\mu_8}{2}T^2\\ &+ \frac{1}{\sigma_7}{e_2}^2 + \left(\frac{1}{\sigma_1} + \frac{\beta}{\sigma_2} + \frac{\beta}{\sigma_3}\right)L\overline{F}^2 < +\infty.\end{aligned} \tag{50}$$

Invoking (44)–(50) obtains

$$\begin{aligned}\dot{\Omega}(t) &\leq -\zeta_1\int_0^L \dot{\kappa}^2 dz - \zeta_2\int_0^L {\alpha''}^2 dz - \zeta_3\int_0^L {\alpha'}^2 dz\\ &\quad - \zeta_4{u_a}^2(t) - \zeta_5\theta_n^2(t) - \zeta_6\tilde{e}_1^2\\ &\quad - \zeta_7\tilde{I}^2 - \zeta_8\tilde{e}_2^2 - \zeta_9\tilde{\bar{r}}^2 + \epsilon\\ &\leq -\gamma_3[\Omega_1(t) + \Omega_2(t) + \eta(t)] + \epsilon\\ &\leq -\gamma\Omega(t) + \epsilon\end{aligned} \tag{51}$$

where $\gamma_3 = \min([2\zeta_1/\rho], (2\zeta_2/EI), (2\zeta_3/T), (2\zeta_4/I), (2\zeta_5/k_\theta), 2\zeta_6, 2\zeta_7, 2\zeta_8, 2\zeta_9)$, and $\gamma = (\gamma_3/\gamma_1)$.

Appendix C

Multiplying (28) by $e^{\gamma t}$ yields

$$\frac{\partial}{\partial t}\left[\Omega(t)e^{\gamma t}\right] \leq \epsilon^{\gamma t}. \tag{52}$$

We then derive

$$\Omega(t) \leq \left[\Omega(0) - \frac{\epsilon}{\gamma}\right]e^{-\gamma t} + \frac{\epsilon}{\gamma}. \tag{53}$$

Invoking (23) and Lemma 2 yields

$$\frac{1}{2L}\beta T\alpha^2 \leq \frac{\beta}{2}T\int_0^L {\alpha'}^2 dz \leq \Omega_1(t) \leq \frac{1}{\gamma_1}\Omega(t). \tag{54}$$

Then, we obtain

$$|\alpha(z,t)| \leq \sqrt{\frac{2L}{\beta T\gamma_1}\left[\Omega(0) + \frac{\epsilon}{\gamma}\right]} \quad \forall z \in [0, L]. \tag{55}$$

We further have

$$\lim_{t\to\infty}|\alpha(z,t)| \leq \sqrt{\frac{2L\epsilon}{\beta T\gamma_1\gamma}} \quad \forall z \in [0, L]. \tag{56}$$

Furthermore, the uniform boundedness of $\theta_n(t)$ is derived as follows:

$$|\theta_n(t)| \leq \sqrt{\frac{2}{k_\theta\gamma_1}\left[\Omega(0) + \frac{\epsilon}{\gamma}\right]} \quad \forall t \in [0, +\infty). \tag{57}$$

Therefore, we deduce

$$\lim_{t\to\infty}|\theta_n(t)| \leq \sqrt{\frac{2\epsilon}{k_\theta\gamma_1\gamma}}. \tag{58}$$

Ultimately, the output states $\alpha(z,t)$ and $\theta_n(t)$ can be ensured to converge to a diminutive neighborhood around 0 by appropriately adjusting the design parameters.

REFERENCES

[1] C. Yang, H. Wu, Z. Li, W. He, N. Wang, and C.-Y. Su, "Mind control of a robotic arm with visual fusion technology," *IEEE Trans. Ind. Informat.*, vol. 14, no. 9, pp. 3822–3830, Sep. 2018.

[2] Z. Li, B. Huang, Z. Ye, M. Deng, and C. Yang, "Physical human–robot interaction of a robotic exoskeleton by admittance control," *IEEE Trans. Ind. Electron.*, vol. 65, no. 12, pp. 9614–9624, Dec. 2018.

[3] S. Yavuz, L. Malgaca, and H. Karagülle, "Vibration control of a single-link flexible composite manipulator," *Composite Struct.*, vol. 140, pp. 684–691, Apr. 2016.

[4] Z. Zhao, Z. Liu, W. He, K.-S. Hong, and H.-X. Li, "Boundary adaptive fault-tolerant control for a flexible Timoshenko arm with backlash-like hysteresis," *Automatica*, vol. 130, Aug. 2021, Art. no. 109690.

[5] Z. Zhao, X. He, and C. K. Ahn, "Boundary disturbance observer-based control of a vibrating single-link flexible manipulator," *IEEE Trans. Syst., Man, Cybern., Syst.*, vol. 51, no. 4, pp. 2382–2390, Apr. 2021.

[6] W. He, T. Wang, X. He, L.-J. Yang, and O. Kaynak, "Dynamical modeling and boundary vibration control of a rigid-flexible wing system," *IEEE/ASME Trans. Mechatronics*, vol. 25, no. 6, pp. 2711–2721, Dec. 2020.

[7] S. Zhang, R. Liu, K. Peng, and W. He, "Boundary output feedback control for a flexible two-link manipulator system with high-gain observers," *IEEE Trans. Control Syst. Technol.*, vol. 29, no. 2, pp. 835–840, Mar. 2021.

[8] Y. Liu, W. Zhan, M. Xing, Y. Wu, R. Xu, and X. Wu, "Boundary control of a rotating and length-varying flexible robotic manipulator system," *IEEE Trans. Syst., Man, Cybern., Syst.*, vol. 52, no. 1, pp. 377–386, Jan. 2022.

[9] N. Jiang, S. Zhang, J. Xu, and D. Zhang, "Model-free control of flexible manipulator based on intrinsic design," *IEEE/ASME Trans. Mechatronics*, vol. 26, no. 5, pp. 2641–2652, Oct. 2021.

[10] K. Li, H. Wang, X. Liang, and Y. Miao, "Visual servoing of flexible-link manipulators by considering vibration suppression without deformation measurements," *IEEE Trans. Cybern.*, vol. 52, no. 11, pp. 12454–12463, Nov. 2022.

[11] W. He, F. Kang, L. Kong, Y. Feng, G. Cheng, and C. Sun, "Vibration control of a constrained two-link flexible robotic manipulator with fixed-time convergence," *IEEE Trans. Cybern.*, vol. 52, no. 7, pp. 5973–5983, Jun. 2022.

[12] T. Chen and J. Shan, "Distributed control of multiple flexible manipulators with unknown disturbances and dead-zone input," *IEEE Trans. Ind. Electron.*, vol. 67, no. 11, pp. 9937–9947, Nov. 2020.

[13] J. Bao, H. Wang, P. X. Liu, and C. Cheng, "Fuzzy finite-time tracking control for a class of nonaffine nonlinear systems with unknown dead zones," *IEEE Trans. Syst., Man, Cybern., Syst.*, vol. 51, no. 1, pp. 452–463, Jan. 2021.

[14] D. Liu, Z. Liu, C. L. P. Chen, and Y. Zhang, "Distributed adaptive neural fixed-time tracking control of multiple uncertain mechanical systems with actuation dead zones," *IEEE Trans. Syst., Man, Cybern., Syst.*, vol. 52, no. 6, pp. 3859–3872, Jun. 2022.

[15] W. He, X. He, and C. Sun, "Vibration control of an industrial moving strip in the presence of input deadzone," *IEEE Trans. Ind. Electron.*, vol. 64, no. 6, pp. 4680–4689, Jun. 2017.

[16] S. Chen, Z. Zhao, D. Zhu, C. Zhang, and H.-X. Li, "Adaptive robust control for a spatial flexible Timoshenko manipulator subject to input dead-zone," *IEEE Trans. Syst., Man, Cybern., Syst.*, vol. 52, no. 3, pp. 1395–1404, Mar. 2022.

[17] Z. Zhao, C. K. Ahn, and H.-X. Li, "Dead zone compensation and adaptive vibration control of uncertain spatial flexible riser systems," *IEEE/ASME Trans. Mechatronics*, vol. 25, no. 3, pp. 1398–1408, Jun. 2020.

[18] J. Zhou, C. Wen, and W. Wang, "Adaptive control of uncertain nonlinear systems with quantized input signal," *Automatica*, vol. 95, pp. 152–162, Sep. 2018.

[19] H. Ma, Q. Zhou, L. Bai, and H. Liang, "Observer-based adaptive fuzzy fault-tolerant control for stochastic nonstrict-feedback nonlinear systems with input Quantization," *IEEE Trans. Syst., Man, Cybern., Syst.*, vol. 49, no. 2, pp. 287–298, Feb. 2019.

[20] Z. Zhao, J. Zhang, Z. Liu, W. He, and K.-S. Hong, "Adaptive quantized fault-tolerant control of a 2-DOF helicopter system with actuator fault and unknown dead zone," *Automatica*, vol. 148, Feb. 2023, Art. no. 110792.

[21] Z. Liu, F. Wang, Y. Zhang, and C. L. Chen, "Fuzzy adaptive quantized control for a class of stochastic nonlinear uncertain systems," *IEEE Trans. Cybern.*, vol. 46, no. 2, pp. 524–534, Feb. 2016.

[22] L. Xing, C. Wen, H. Su, Z. Liu, and J. Cai, "Robust control for a class of uncertain nonlinear systems with input quantization," *Int. J. Robust Nonlinear. Control*, vol. 26, no. 8, pp. 1585–1596, 2016.

[23] T. Zanma, T. Ohtsuka, and K.-Z. Liu, "Set-based state estimation in quantized state feedback control systems with quantized measurements," *IEEE Trans. Control Syst. Technol.*, vol. 28, no. 2, pp. 550–557, Mar. 2020.

[24] S. Gao and J. Liu, "Adaptive neural network vibration control of a flexible aircraft wing system with input signal quantization," *Aerosp. Sci. Technol.*, vol. 96, Jan. 2020, Art. no. 105593.

[25] J. Wang and J. Liu, "Event-triggered boundary quantization control for flexible manipulator based on partial differential equations dynamic model," *Trans. Inst. Meas. Control*, vol. 43, no. 9, pp. 2111–2123, 2021.

[26] J. Wang and J. Liu, "Bilateral coordination quantisation control for master–slave flexible manipulators based on PDE dynamic model," *Int. J. Control*, vol. 95, no. 8, pp. 2279–2292, 2021.

[27] W. He, Y. Ouyang, and J. Hong, "Vibration control of a flexible robotic manipulator in the presence of input deadzone," *IEEE Trans. Ind. Informat.*, vol. 13, no. 1, pp. 48–59, Feb. 2017.

[28] W. He, X. He, M. Zou, and H. Li, "PDE model-based boundary control design for a flexible robotic manipulator with input backlash," *IEEE Trans. Control Syst. Technol.*, vol. 27, no. 2, pp. 790–797, Mar. 2019.

[29] M. Polycarpou and P. Ioannou, "A robust adaptive nonlinear control design," *Automatica*, vol. 32, no. 3, pp. 423–427, 1996.

[30] J. Zhou, C. Wen, W. Wang, and F. Yang, "Adaptive backstepping control of nonlinear uncertain systems with quantized states," *IEEE Trans. Autom. Control*, vol. 64, no. 11, pp. 4756–4763, Nov. 2019.

[31] *Srv02 User Manual*, Quanser, Inc., Markham, ON, Canada, 2009.

[32] X. He, S. Zhang, Y. Ouyang, and Q. Fu, "Vibration control for a flexible single-link manipulator and its application," *IET Control Theory Appl.*, vol. 14, no. 7, pp. 930–938, 2020.

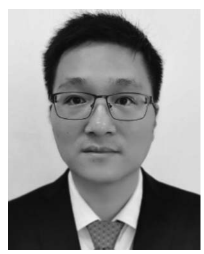

Zhijia Zhao (Member, IEEE) received the B.Eng. degree in automatic control from the North China University of Water Resources and Electric Power, Zhengzhou, China, in 2010, and the M.Eng. and Ph.D. degrees in automatic control from the South China University of Technology, Guangzhou, China, in 2013 and 2017, respectively.

He is currently an Associate Professor with the School of Mechanical and Electrical Engineering, Guangzhou University, Guangzhou. His research interests include adaptive and learning control, flexible mechanical systems, and robotics.

Yiming Liu received the B.Eng. degree in robotics engineering from Guangzhou University, Guangzhou, China, in 2021, where he is currently pursuing the master's degree in control science and engineering.

His research interests include flexible systems, distributed parameter system control, and robotics.

Sentao Cai received the B.Eng. degree in electrical engineering and automation from Guangzhou University, Guangzhou, China, in 2020, where he is currently pursuing the master's degree in control science and engineering.

His research interests include flexible systems and adaptive control.

Zhifu Li (Member, IEEE) received the B.Sc. and M.Sc. degrees in control theory and control engineering from Central South University, Changsha, Hunan, China, in 2003 and 2006, respectively, and the Ph.D. degree in control theory and control engineering from the South China University of Technology, Guangzhou, Guangdong, China, in 2012.

From 2012 to 2015, he was a Postdoctoral Fellow of Mechatronics with the South China University of Technology. He has been with the School of Mechanical and Electrical Engineering, Guangzhou University, Guangzhou, since 2015, where he is currently an Associate Professor. He has published over 30 research articles. His research interests include nonlinear control and its application, swarm intelligence optimization, applied fractional calculus, robust adaptive control, and machine vision.

Yiwen Wang (Senior Member, IEEE) received the Ph.D. degree from the University of Florida, Gainesville, FL, USA, in 2008. She is an Associate Professor with the Department of Electronic and Computer Engineering and the Department of Chemical and Biological Engineering, The Hong Kong University of Science and Technology, Hong Kong, where she is currently an Associate Professor with substantiation. She holds two U.S. patents and has authored more than 100 peer-reviewed publications. Her research interests are in neural decoding of brain–machine interfaces, adaptive signal processing, computational neuroscience, and neuromorphic engineering.

Dr. Wang serves as the Chair of the IEEE EMBS Neural Engineering Tech Committee, the Chair of the IEEE BRAIN Publication Subcommittee, and the Board Member of the Brain Computer Interfaces Society. She is the Editor-in-Chief of the IEEE BRAIN NEWSLETTER. She also serves on the editorial board of the *Journal of Neural Engineering*, and is the Associate Editor of *Frontiers in Human Neuroscience* (Brain Computer Interfaces), the IEEE TRANSACTIONS ON NEURAL SYSTEMS AND REHABILITATION ENGINEERING, and the IEEE TRANSACTIONS ON COGNITIVE AND DEVELOPMENTAL ENGINEERING. She was recognized as an IEEE EMBS Distinguished Lecturer in 2022.

Keum-Shik Hong (Fellow, IEEE) received the B.S. degree in mechanical design from Seoul National University, Seoul, South Korea, in 1979, the M.S. degree in mechanical engineering from Columbia University, New York, NY, USA, in 1987, and the M.E. degree in applied mathematics and the Ph.D. degree in mechanical engineering from the University of Illinois at Urbana–Champaign, Champaign, IL, USA, in 1991 and 1997, respectively.

He joined the School of Mechanical Engineering, Pusan National University, Busan, South Korea, in 1993. His research interests include brain–computer interface, nonlinear systems theory, adaptive control, and distributed parameter systems.

Dr. Hong has received many awards, including the Best Paper Award from the KFSTS of Korea in 1999 and the Presidential Award of Korea in 2007. He served as an Associate Editor for *Automatica* from 2000 to 2006 and the Editor-in-Chief for the *Journal of Mechanical Science and Technology* from 2008 to 2011, and serving as the Editor-in-Chief for the *International Journal of Control, Automation, and Systems*. He was the past President of the Institute of Control, Robotics and Systems (ICROS), South Korea, and the President of the Asian Control Association. He is a Fellow of the Korean Academy of Science and Technology, an ICROS Fellow, and a member of the National Academy of Engineering of Korea.

Han-Xiong Li (Fellow, IEEE) received the B.E. degree in aerospace engineering from the National University of Defense Technology, Changsha, China, in 1982, the M.E. degree in electrical engineering from the Delft University of Technology, Delft, The Netherlands, in 1991, and the Ph.D. degree in electrical engineering from the University of Auckland, Auckland, New Zealand, in 1997.

He is currently a Chair Professor with the Department of SEEM, City University of Hong Kong, Hong Kong. He has a broad experience in both academia and industry. He has authored two books and about 20 patents and has published more than 200 SCI journal articles with H-index 55 (Web of Science). His current research interests include process modeling and control, system intelligence, distributed parameter systems, and battery management systems.

Dr. Li was awarded the Distinguished Young Scholar (overseas) by the China National Science Foundation in 2004, a Chang Jiang Professorship by the Ministry of Education, China, in 2006, and a National Professorship in China Thousand Talents Program in 2010. He serves as a Distinguished Expert for Hunan Government and China Federation of Returned Overseas Chinese. He serves as an Associate Editor for IEEE TRANSACTIONS ON SYSTEMS, MAN, AND CYBERNETICS: SYSTEMS and was an Associate Editor for IEEE TRANSACTIONS ON CYBERNETICS from 2002 to 2016 and IEEE TRANSACTIONS ON INDUSTRIAL ELECTRONICS from 2009 to 2015.